Corrections

GENETICS. For the article "A common variant in combination with a nonsense mutation in a member of the thioredoxin family causes primary ciliary dyskinesia," by Bénédicte Duriez, Philippe Duquesnoy, Estelle Escudier, Anne-Marie Bridoux, Denise Escalier, Isabelle Rayet, Elisabeth Marcos, Anne-Marie Vojtek, Jean-François Bercher, and Serge Amselem, which appeared in issue 9, February 27, 2007, of *Proc Natl Acad Sci USA* (104:3336–3341; first published February 20, 2007; 10.1073/pnas.0611405104), Fig. 1 appeared incorrectly, due to a printer's error. The online version has been corrected. The corrected figure and its legend appear below.

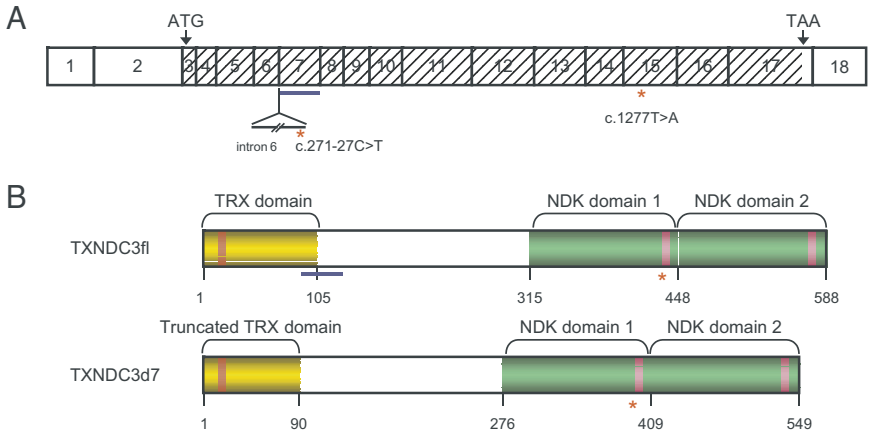

Fig. 1. The human *TXNDC3* gene and related products. (*A*) *TXNDC3* cDNA structure showing the location of the exons drawn to scale. The translation start and stop codons are labeled with ATG and TAA, respectively. The translated region is hashed. Exon 7 is underlined in blue, and intron 6 is shown as a thin line below exons 6 and 7. The red asterisks mark the locations of the c.271–27C>T and c.1277T>A nucleotide variations, located in intron 6 and exon 15, respectively. (*B*) Structure of the TXNDC3 isoforms: the TXNDC3fl isoform (*Upper*) and the TXNDC3d7 isoform (*Lower*). The thioredoxin (TRX) domain and the two NDK domains are shown in yellow and green, respectively. Within the TRX domain, the active site (GCPC) is shown by an orange box, and, within the NDK domains, the putative NDP kinase active sites are shown by pink boxes. The location of the region encoded by exon 7 is underlined in blue. The location of the p.Leu426X mutation is shown by a red asterisk.

www.pnas.org/cgi/doi/10.1073/pnas.0702345104

APPLIED BIOLOGICAL SCIENCES. For the article "An *in vitro* and *in vivo* disconnect uncovered through high-throughput identification of botulinum neurotoxin A antagonists," by Lisa M. Eubanks, Mark S. Hixon, Wei Jin, Sukwon Hong, Colin M. Clancy, William H. Tepp, Michael R. Baldwin, Carl J. Malizio, Michael C. Goodnough, Joseph T. Barbieri, Eric A. Johnson, Dale L. Boger, Tobin J. Dickerson, and Kim D. Janda, which appeared in issue 8, February 20, 2007, of *Proc Natl Acad Sci USA* (104:2602–2607; first published February 9, 2007; 10.1073/pnas.0611213104), the authors note that, due to a printer's error, the following statement was omitted from the Acknowledgments: "We also thank Laura A. McAllister, Jack P. Kennedy, and Grant E. Boldt (all of The Scripps Research Institute, La Jolla, CA) for providing the 2,4-dichlorocinnamic hydroxamic acid."

www.pnas.org/cgi/doi/10.1073/pnas.0702406104

MEDICAL SCIENCES. For the article "c-Myc-mediated genomic instability proceeds via a megakaryocytic endomitosis pathway involving Gp1bα," by Youjun Li, Jie Lu, and Edward V. Prochownik, which appeared in issue 9, February 27, 2007, of *Proc Natl Acad Sci USA* (104:3490–3495; first published February 20, 2007; 10.1073/pnas.0610163104), the authors note that, due to a printer's error, the curves in several panels of Fig. 4 were shifted to the left. The corrected figure and its legend appear below. This error does not affect the conclusions of the article.

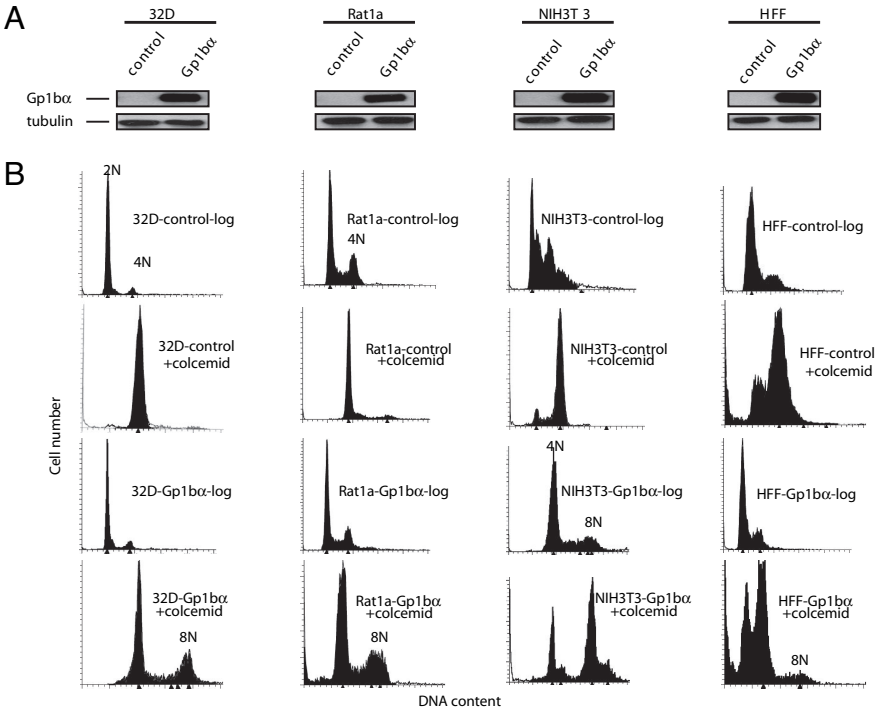

Fig. 4. Enforced expression of Gp1bα is sufficient for the induction of tetraploidy in various cell types. Stable expression of Gp1bα in the indicated immortalized or primary cells was accomplished through transduction with a bicistronic LXSN retroviral vector expressing myc-epitope-tagged Gp1bα and enhanced yellow fluorescent protein (EYFP, ref. 23). Control cell lines were derived after transduction with the empty parental vector. In both cases, pure populations of EYFP-positive cells were obtained by fluorescence-activated cell sorting (23). (*A*) Immunoblotting for Gp1bα and tubulin expression after expansion of EYFP-positive cells. (*B*) Cell cycle analyses. The indicated cells were examined during log-phase growth or after exposure to colcemid. Similar results were seen after stable transfection of several cell lines with a pcDNA-based, nonepitope-tagged Gp1bα expression vector, thus indicating that the method of delivery, the nature of the vector, and the presence of an epitope tag were not important for conferring the tetraploid genotype (data not shown and Fig. 3 *B–D*).

www.pnas.org/cgi/doi/10.1073/pnas.0702407104

An *in vitro* and *in vivo* disconnect uncovered through high-throughput identification of botulinum neurotoxin A antagonists

Lisa M. Eubanks*[†‡], Mark S. Hixon*[†‡], Wei Jin*[†], Sukwon Hong*[†], Colin M. Clancy[§], William H. Tepp[§], Michael R. Baldwin[¶], Carl J. Malizio[‖], Michael C. Goodnough[‖], Joseph T. Barbieri[¶], Eric A. Johnson[§], Dale L. Boger*[†], Tobin J. Dickerson*[†‡]**, and Kim D. Janda*[†‡]**[††]

Departments of *Chemistry and [††]Immunology, [†]The Skaggs Institute for Chemical Biology, and [‡]The Worm Institute of Research and Medicine, The Scripps Research Institute, 10550 North Torrey Pines Road, La Jolla, CA 92037; [§]Food Research Institute, University of Wisconsin, 1925 Willow Drive, Madison, WI 53706; [¶]Department of Microbiology and Molecular Genetics, Medical College of Wisconsin, 8701 Watertown Plank Road, Milwaukee, WI 53226; and [‖]Metabiologics, 505 South Rosa Road, Madison, WI 53719

Communicated by Sydney Brenner, The Salk Institute for Biological Studies, La Jolla, CA, December 18, 2006 (received for review December 7, 2006)

Among the agents classified as ''Category A'' by the U.S. Centers for Disease Control and Prevention, botulinum neurotoxin (BoNT) is the most toxic protein known, with microgram quantities of the protein causing severe morbidity and mortality by oral or i.v. routes. Given that this toxin easily could be used in a potential bioterrorist attack, countermeasures urgently are needed to counteract the pathophysiology of BoNT. At a molecular level, BoNT exerts its paralytic effects through intracellular cleavage of vesicle docking proteins and subsequent organism-wide autonomic dysfunction. In an effort to identify small molecules that would disrupt the interaction between the light-chain metalloprotease of BoNT serotype A and its cognate substrate, a multifaceted screening effort was undertaken. Through the combination of *in vitro* screening against an optimized variant of the light chain involving kinetic analysis, cellular protection assays, and *in vivo* mouse toxicity assays, molecules that prevent BoNT/A-induced intracellular substrate cleavage and extend the time to death of animals challenged with lethal toxin doses were identified. Significantly, the two most efficacious compounds *in vivo* showed less effective activity in cellular assays intended to mimic BoNT exposure; indeed, one of these compounds was cytotoxic at concentrations three orders of magnitude below its effective dose in animals. These two lead compounds have surprisingly simple molecular structures and are readily amenable to optimization efforts for improvements in their biological activity. The findings validate the use of high-throughput screening protocols to define previously unrecognized chemical scaffolds for the development of therapeutic agents to treat BoNT exposure.

bioterrorism | high-throughput screening | small molecule inhibitors

Botulinum neurotoxins (BoNTs) are the etiological agents responsible for botulism, a disease characterized by peripheral neuromuscular blockade and a characteristic flaccid paralysis in humans. Seven serologically distinguishable serotypes of the neurotoxin (A–G) are produced and secreted by the rod-shaped, Gram-positive, sporulating anaerobic bacillus *Clostridium botulinum* as well as by neurotoxigenic strains of *Clostridium butyricum* and *Clostridium baratii* (1). BoNTs are synthesized as inactive ≈150-kDa single-chain proteins that are activated by proteolytic cleavage to form a disulfide-linked dimer consisting of a 100-kDa heavy chain and a 50-kDa light chain (LC), depending on the serotype (2, 3). While the heavy chain comprises the receptor binding and translocation domains, the LC is a Zn^{2+}-dependent endopeptidase that exclusively cleaves at specific sites one of three intracellular soluble *N*-ethylmaleimide-sensitive factor attachment protein receptor (SNARE) proteins: synaptosomal-associated protein of 25 kDa (SNAP-25), vesicle-associated membrane protein (VAMP)/synaptobrevin, or syntaxin. As a result of this cleavage event, the neural exocytosis docking/fusion machinery becomes impaired, and the release of acetylcholine at the neuromuscular junction is inhibited, leading to loss of neurotransmission. In severe cases of botulism, this molecular event results in neuronal paralysis, subsequent impaired respiratory function, and autonomic dysfunction. BoNT/A is the deadliest of the seven toxins with a potency ≈100 billion times that of cyanide (4); the lethal dose for humans is ≈1 ng/kg of body weight (5).

Despite an increasing number of clinical disorders relying on BoNT/A, including strabismus, blepharospasm, and hemifacial spasm, as well as a number of other maladies such as migraines and wrinkles (6, 7), this deadly poison still is classified by the Centers for Disease Control and Prevention (CDC) as being one of six highest-risk agents for bioterrorism (''Category A'' agent). Because of ease of production, exceptional potency, and long duration of paralysis, BoNT/A is the most likely serotype to be deployed during a biological assault. Although no approved pharmacological treatments exist for adult botulism, human botulism immune globulin intravenous (BIG-IV) has been shown to neutralize BoNT in infant cases and may prove to have efficacy in other scenarios (8). However, the availability of the human-derived immunoglobulins from immunized personnel is extremely limited. The most effective immunotherapy for protection against BoNTs relies on vaccination with pentavalent toxoid species, although supplies are reserved for high-risk individuals (9). Alternate countermeasures are limited to the passive administration of antibodies, which are expensive to produce in large enough quantities necessary to combat a bioterrorism attack, are currently of equine origin that can cause serious side effects, and have only a very short window of application. Furthermore, once BoNTs begin entry into the neuronal cell, antitoxins become ineffective. Clearly, a pharmacotherapeutic displaying effective neutralization of the clinical symptoms of botulism is critical in response to widespread BoNT exposure.

Small molecules provide an opportunity to treat botulism both before and after cellular intoxication has occurred. Over the past decade, inhibitors of the BoNT LC/A zinc metalloprotease have emerged as the most popular target in BoNT drug discovery (10). BoNT LC/A cleaves the intracellular SNARE protein SNAP-25, thereby preventing the fusion of synaptic vesicles to the plasma

Author contributions: L.M.E., M.S.H., E.A.J., T.J.D., and K.D.J. designed research; L.M.E., M.S.H., W.J., S.H., C.M.C., W.H.T., C.J.M., and M.C.G. performed research; W.J., S.H., M.R.B., J.T.B., and D.L.B. contributed new reagents/analytic tools; L.M.E., M.S.H., E.A.J., D.L.B., and T.J.D. analyzed data; and L.M.E., T.J.D., and K.D.J. wrote the paper.

The authors declare no conflict of interest.

Abbreviations: BoNT, botulinum neurotoxin; LC, light chain; SNAP-25, synaptosomal-associated protein of 25 kDa.

**To whom correspondence may be addressed. E-mail: kdjanda@scripps.edu or tobin@scripps.edu.

www.pnas.org/cgi/doi/10.1073/pnas.0611213104

membrane of neurons containing the receptors for BoNT/A. One approach has taken advantage of peptide-based inhibitors that mimic portions of the natural substrate, SNAP-25, and compete for binding to the enzyme active site (11). A complementary approach used by our laboratory and others has focused on metal chelators, which presumably bind the active site zinc cation, thereby rendering the BoNT LC inactive (12–14). Analogous to these approaches, others have used an *in silico* screen of a large compound library in an effort to identify BoNT/A-selective inhibitors and establish a pharmacophore for BoNT/A LC inhibition; again, the most effective compounds identified by using this approach operated by zinc chelation (15, 16). However, it is important to note that this pharmacophore has been established from *in vitro* methods, with scant *in vivo* data for any reported compound. In the absence of a defined model for predicting *in vivo* efficacy, we initiated a multifaceted research program aimed at identifying novel small-molecule inhibitors of BoNT LC/A through a three-step sequential process: (*i*) a high-throughput screen using optimized recombinant LC/A, (*ii*) evaluation of the best candidates in a cell-based model, and (*iii*) *in vivo* testing in a murine toxicity bioassay.

Results and Discussion

High-Throughput Screening and Preliminary Cellular Assays. In the wake of the events of September 11, 2001, research efforts aimed at the discovery of potent antagonists for agents of bioterrorism have increased exponentially. However, despite the plethora of new data that has emerged in the past 5 years, an established pharmacophore validated through *in vivo* models of exposure remains elusive. Indeed, in the case of BoNT, scant studies have reported the assessment of any small molecule antagonist in animal models (17, 18).

The catalytic LC domain of BoNT/A is a compact globule consisting of a mixture of α-helices, β-sheets, and β-strands with a zinc-containing metalloprotease active site bound deeply inside a large open cavity (2). The remarkable substrate selectivity of BoNT/A for SNAP-25 has been explained to be a consequence of extensive interactions with two exosite domains distinct from the active site (19). A model for substrate recognition has been proposed in which α-exosite binding occurs first via helix formation in the appropriate region of SNAP-25, followed by β-exosite recognition and subsequent conformational changes in the enzyme to facilitate efficient substrate cleavage (19). This model argues that, without exosite binding, BoNT/A is a significantly less efficient enzyme, and thus these regions could be targeted for lead development.

The interaction between BoNT/A and its cognate substrate can be viewed simply as a series of protein–protein interactions that ultimately result in a catalytic event. The study of small molecules that disrupt protein–protein interactions has evolved into a rich area, with molecules demonstrated to interrupt numerous systems of clinical significance (20–23). It generally is accepted that the structural stability of protein–protein interactions derives from large, but relatively shallow, interfaces (24–27) and that the difficulty in antagonizing interactions on such a large molecular scale has been linked to the size of the buried hydrophobic surfaces. A key insight occurred in this field with the identification of "hot spots" (28, 29), domains characterized as shallow loci of $\approx$600 Å^2 found on the surface of a protein. In general, these areas are found at or near the geometric center of the protein–protein interface, and certain amino acids in hot spot regions contribute significantly to the stability of protein–protein complexes. In particular, the amino acids tryptophan, tyrosine, and histidine, as well as other hydrophobic residues, are represented (30, 31).

Given the presence of a critical protein–protein interaction in the mechanism of BoNT LC/A catalytic activity, we hypothesized that small molecule antagonists could be identified from a high-throughput screen of a large set of compounds with demonstrated activity in disrupting protein–protein interactions. The Boger laboratory previously has reported a collection of such libraries (21) consisting of $\approx$66,000 compounds prepared by using solution phase technology with liquid–liquid acid–base extraction purification (32). Screening was conducted by using a recombinant, truncated form of the catalytic domain of BoNT/A, termed LC/A (1–425). In this enzyme, the C-terminal 23 aa have been deleted to produce a soluble and stable version of the enzyme that easily can be expressed in *Escherichia coli* at high levels and purified in large quantities necessary for a screening on this scale (33). LC/A catalytic activity was measured by using a fluorescence resonance energy transfer (FRET) assay in a rapid 96-well plate format (12) with compounds present in pools of 3–10 members to maximize screening efficiency. Although we recognize that this screening could potentially result in false positives as a consequence of tertiary or greater interactions in solution, this procedure allows a single researcher to evaluate the entire library in as little as 1 month without the need for automation.

Table 1. IC_{50} values for pools of compounds screened against LC/A (1–425)

Compounds	Pool size	IC_{50}, μM
29A7 (BBF-AB11C7)*	10	14.8
5G7 (HD1c-A1B7Cm2)†	8	16.9
14E2 (FA-A2B2C)	3	15.8
39G6 (TransPyr1-A1B6Cm1)	10	13.0
40D9 (TransPyr1-A6B9Cm1)	10	19.3
40H6 (TransPyr1-A10B6Cm1)	10	19.8
42F6 (TransPyr1-A4B6Cm3)	10	16.2
43C7 (TransPyr1-A9B7Cm3)	10	11.1

Assays were conducted at varied concentration of the pooled inhibitors at 23°C, pH 7.4, in 40 mM Hepes, 5 μM SNAPtide, and 7 nM LC/A.
*See ref. 47 for library preparation.
†See ref. 48 for library preparation.

The initial library screen resulted in eight compound pools displaying apparent IC_{50} values of $\leq$20 μM (Table 1). Before deconvolution of these promising pools, potency was evaluated by a secondary screening process to further narrow the number of potential inhibitors and putatively bolster the likelihood of *in vivo* efficacy. The LC of BoNT/A cleaves the C-terminal 9 aa residues of SNAP-25, thereby producing an $\approx$24-kDa degradation protein (34). Analytical techniques have been developed that directly assess SNAP-25 cleavage in cell lysates by using immunoelectrophoresis (35). Using this method, we analyzed the amount of intact versus cleaved SNAP-25 allowing correlation to LC/A activity/inhibition within a Neuro-2a cellular model. In the absence of toxin, SNAP-25 remains fully intact (Fig. 1*A*, − control), and in the presence of toxin, a lower-molecular-weight proteolysis product (Fig. 1*A*, + control) is observed. Pools 39G6, 40D9, and 42F6 were partially protective with a decrease in cleaved SNAP-25 of $\approx$49–57%, and pool 40H6 displayed total protection with only full-length SNAP-25 visible (Fig. 1*B*). In addition, by employing a cellular secondary screen, cytotoxic compounds could be removed at an early stage from further consideration (pool 5G7). Encouraged by the results of the primary and secondary screens, we proceeded to deconvolute these promising pools for further evaluation.

Single-Compound Evaluation. After each lead pool was deconvoluted into individual compounds by parallel synthesis, single compounds were tested against recombinant BoNT LC/A by using the previously described FRET assay. Although many of the individual compounds displayed poor or no activity in this assay, a group of 12 inhibitors with IC_{50} values ranging from $\approx$1–90 μM was selected as the most promising candidates and reexamined in cellular studies (Table 2). In the Neuro-2a cell-based assay, protection from intracellular SNAP-25 cleav-

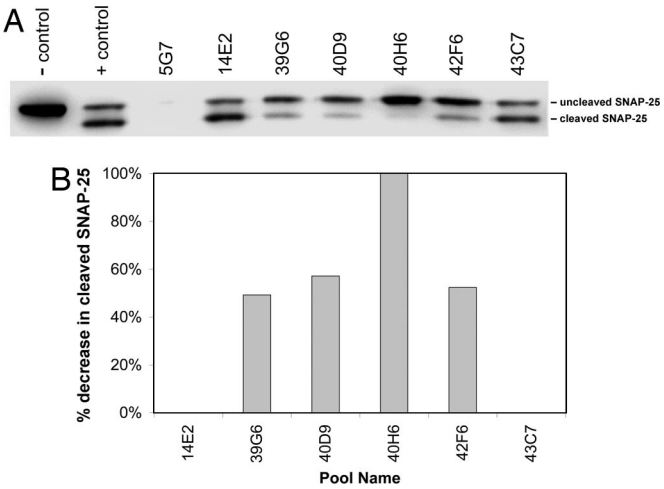

Fig. 1. Evaluation of potential small molecule inhibitors of BoNT/A in a cellular model. (*A*) Inhibition of SNAP-25 cleavage in a Neuro-2a cell assay. (*B*) Bar graph illustrating the percentage decrease in cleaved SNAP-25, correlating to the amount of cellular protection. Each entry represents a pool of compounds tested at a total concentration of 50 μM.

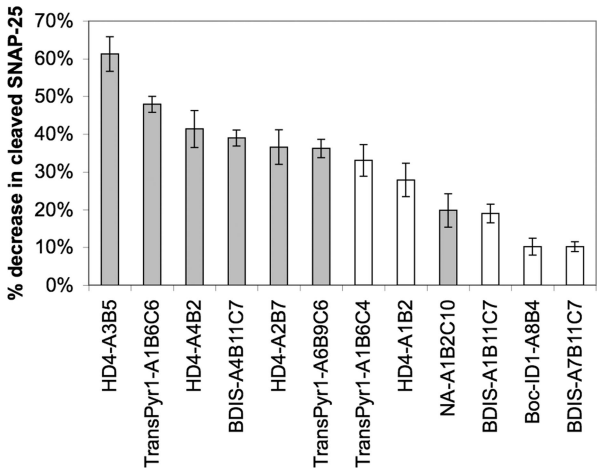

Fig. 2. Inhibition of SNAP-25 cleavage in a Neuro-2a cell assay displayed as the percentage decrease in cleaved SNAP-25, correlating to the amount of cellular protection (filled bars signify inhibitors studied further *in vivo*). All compounds were tested at a concentration of 25 μM.

age was as high as 61% for the most potent compound, HD4-A3B5, and as low as 10% for the least potent compound, BDIS-A7B11C7 (Fig. 2). Disappointingly, pool 40H6, which initially showed complete protection of SNAP-25 cleavage in initial cellular assays (Fig. 1), provided no individual members with efficacy in either the FRET or the cell-based assay up to a concentration of 250 μM. We speculate that the activity observed in initial screening was a result of multiple members of the pool operating in concert to inhibit BoNT LC/A; kinetically, this system no longer can be considered simple inhibition and, when extrapolated into cellular models, quickly becomes intractable. Therefore, these compounds were eliminated from further study.

Although we acknowledge that our current studies do not definitively prove exosite inhibitor binding, it is unclear at this time what kinetic model (e.g., competitive, noncompetitive, mixed-type) would appropriately describe this complex enzymatic system. Based on structural evidence and the proposed mechanism of BoNT LC/A catalysis, exosite binding is anticipated to alter the conformation of the enzyme active site (19), and thus, compounds that antagonize this interaction may appear as competitive inhibitors. Additionally, the loss of exosite binding by the natural substrate decreases the rate of catalysis of the enzyme and may cause the reaction to proceed through an alternate and entirely distinct kinetic pathway, leading to the observation of apparent mixed-type inhibition. Furthermore, given that the SNAPtide substrate used in our screen does not explicitly contain the entire α-exosite binding motif, plausible kinetic models can be envisioned in which small molecule binding to the exosite alternatively may lead to enzyme activation relative to substrate alone. Thus, structural studies will be required to definitively distinguish the site of binding and mode of inhibition based on the current assay.

Table 2. IC_{50} values for the most active single compounds screened against LC/A (1–425)

Compound	IC_{50}, μM
Boc-ID1-A8B4*	1.1
BDIS-A1B11C7†	1.5
HD4-A1B2	5.1
HD4-A2B7	7.6
NA-A1B2C10‡	12.5
HD4-A3B5	14.3
BDIS-A7B11C7†	15.4
HD4-A4B2	19.1
TransPyr1-A1B6C4	28.4
TransPyr1-A1B6C6	54.2
BDIS-A4B11C7†	46.2
TransPyr1-A6B9C6	91.2

Assays were conducted at varied concentration of inhibitors at 23°C, pH 7.4, in 40 mM Hepes, 5 μM SNAPtide, and 7 nM LC/A.
*See ref. 48 for synthetic preparation.
†See ref. 47 for synthetic preparation.
‡See ref. 49 for synthetic preparation.

***In Vivo* Examination of Lead Compounds.** A true test or ultimate goal for inhibitors evaluated in both cell-free systems and cell-based assays is whether their effectiveness holds true *in vivo*. After completion of our two-phase, *in vitro* screening and cellular inhibition studies, seven compounds were deemed to have suitable activity and were advanced into animal models (Fig. 3). Six inhibitors were selected solely based on the extent of SNAP-25 protection in Neuro-2a cells (Fig. 2, filled bars). Although NA-A1B2C10 only provided moderate protection, its relatively simple chemical structure allows for the facile synthesis of this compound; hence, its activity could be anticipated to be improved through the use of traditional medicinal chemistry techniques. In addition, NA-A1B2C10 was deemed the most "drug-like" of all lead compounds in that it meets "the rule of 5" as popularized by Lipinski *et al*. (36). The eighth compound, included for comparison, was a molecule previously reported by our laboratory and designed to inhibit BoNT LC/A through chelation of the active site zinc ion (13). This compound, 2,4-dichlorocinnamic hydroxamic acid (Fig. 3), was found to be toxic to Neuro-2a cells at concentrations $\geq$5 μM and, when analyzed at lower concentrations, showed no reduction in SNAP-25 cleavage relative to control experiments.

To examine the lead compounds *in vivo*, a well established mouse toxicity bioassay was used. This model is the Food and Drug Administration (FDA) standard for assessing BoNT levels and the universally accepted method for the study of BoNT antagonists (e.g., antibodies, small molecules) (37). For testing, animals were challenged with BoNT/A at a dose of $\approx$5–10 times the i.p. LD_{50}. Inhibitors were injected intravenously into test animals immediately after the toxin. All animals were monitored

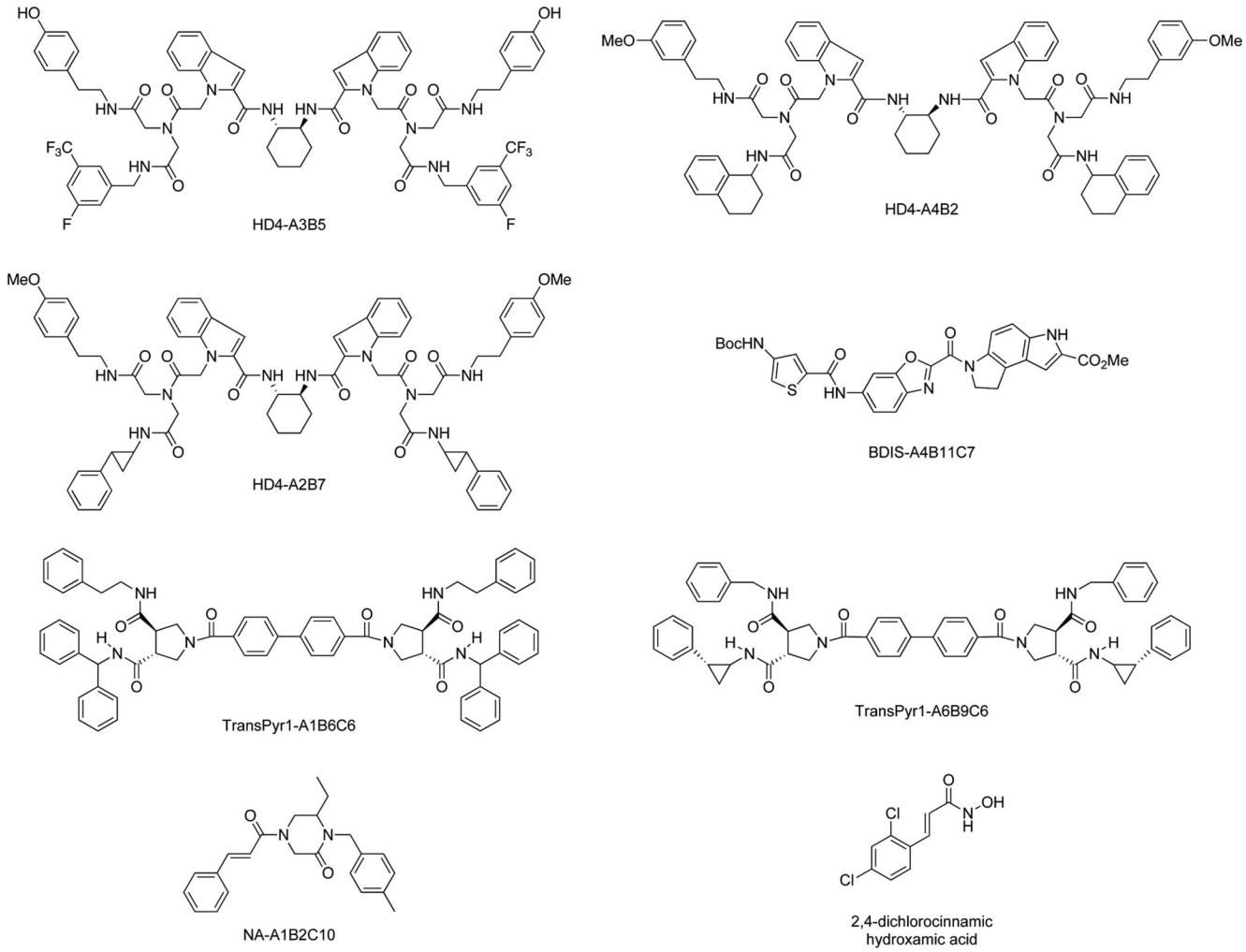

Fig. 3. Chemical structures of single-compound inhibitors progressed to animal studies.

continuously for a period of 12–24 h for signs of botulism, and the time of death was recorded. Of the compounds studied, two compounds, NA-A1B2C10 and 2,4-dichlorocinnamic hydroxamic acid, showed some efficacy in preventing BoNT-induced death. At an injection dosage of 2.5 mM, NA-A1B2C10 extended the time to death from 484 min to 659 min, corresponding to a 36% increase in time to death. Although appearing modest at first glance, this enhancement is remarkable considering its simple molecular structure. In contrast, 16% of animals (5 of 31 mice) treated with 2,4-dichlorocinnamic hydroxamic acid at a dose of 1 mM survived the BoNT challenge indefinitely with no obvious signs of botulism; interestingly, of those animals treated with compound that did die, no statistically significant increase in the time to death was observed relative to control groups. In all cases, no toxicity was observed from treatment with either inhibitor compound alone.

It is critical to note that the two compounds that provided meaningful extension of time to death in animals would not have been predicted from the cellular models. Indeed, one compound (NA-A1B2C10) showed the least protection of SNAP-25 cleavage in cellular assays at 25 μM, whereas the other (2,4-dichlorocinnamic hydroxamic acid) was found to be cytotoxic in neuroblastoma cells at concentrations three orders of magnitude less than those tested in animals (i.e., 5 μM). Numerous cell-based assays have been developed for assessing BoNT toxicity, including cultured murine neuroblastoma cells (Neuro-2a) (38), primary rodent fetal spinal cord cells (35, 39, 40), cultured chicken spinal motor neurons (16), and rat adrenal pheochromocytoma cells (PC12) (41). One of the major advantages of a secondary screen such as cell-based assays is a considerable reduction in the number of animals used, time expended, and cost incurred, especially when used for assessing large numbers of target molecules. However, our findings argue that in the context of BoNT therapeutics, caution should be used in extrapolating *in vivo* potency from these assays because no correlation was evident between cellular activity and *in vivo* efficacy. Although certain aspects of an *in vivo* screen cannot adequately be represented in any cellular assay, including metabolism, clearance, absorption, and distribution, clearly, conducting a high-throughput screen of a large compound library in a mouse bioassay is not feasible. Given the urgent need for botulism treatments that remain operative after BoNT has internalized into peripheral neurons, these studies cogently contend that greater research is needed toward the development of *in vitro* cellular systems that allow for the rapid identification of BoNT antagonists while also accurately depicting the *in vivo* condition.

Our results demonstrate the ability of a multidisciplinary parallel screening program to culminate in the identification of small molecules with *in vivo* antibotulinal activity. Indeed, by employing an unbiased approach, we have discovered previously unconsidered molecular structures that lack characteristic zinc chelation motifs. Furthermore, given the molecular structure of lead compounds

such as NA-A1B2C10 and 2,4-dichlorocinnamic hydroxamic acid, optimization of both *in vitro* inhibitory activity as well as *in vivo* potency readily can be envisioned through the use of traditional structure–activity relationship studies. We propose that compounds such as NA-A1B2C10 and 2,4-dichlorocinnamic hydroxamic acid could be used as a "combination" therapy approach in which multiple compounds would be administered with complementary activities, one component inhibiting BoNT via chelation of the critical zinc atom of the protease while another component prevents BoNT function by disruption of essential protein–protein interactions within the toxin. In total, this study validates the value of high-throughput screening efforts in the discovery of unrecognized targets for combating agents of bioterrorism.

Materials and Methods

Expression and Purification of LC/A (1–425). Recombinant *C. botulinum* LC/A (1–425) was expressed in *E. coli* [pLC 1–425/BL21 RIL (DE3)] and purified by Ni^{+2}-nitrilotriacetic acid affinity chromatography followed by gel filtration (Sephacryl S200 HR) and anion-exchange chromatography (DEAE-Sephacel) as described in ref. 33. Protein concentrations were measured by Coomassie staining with BSA as a standard.

Evaluation of Inhibitors with Recombinant LC/A (1–425). LC/A (1–425) activity was measured in black 96-well microtiter plates (CoStar; Corning, Inc., Corning, NY) by use of a Molecular Devices (Sunnyvale, CA) SpectraMax GeminiEM plate reader. Stock solutions of inhibitors were prepared as 5 mM stocks in DMSO and diluted appropriately. Assays contained 40 mM Hepes (pH 7.4), 7 nM enzyme, and varying concentrations of inhibitor in a final volume of 100 μl. Assay mixtures were preincubated for 5 min at 23°C and were initiated by the addition of 5 μM SNAPtide (List Biological Laboratories, Inc., Campbell, CA). Fluorimeter parameters consisted of a λ_{ex} = 490 nm (slit width = 2 nm), a λ_{em} = 532 nm (slit width = 2 nm), and a cut-off filter at 495 nm. Initial rates were measured from the linear region of each assay, typically from data collected over a range of 100 to 300 s. IC_{50} values were determined by using Eq. **1**, where $[I]$ is the concentration of inhibitor, V_o is the initial rate in the absence of inhibitor, and V is the initial rate in the presence of inhibitor.

$$IC_{50} = \frac{[I]\dfrac{V}{V_0}}{1 - \dfrac{V}{V_0}} . \qquad [1]$$

Cell-Based Assays. Cellular protection against BoNT/A with selected compounds was investigated by using the murine cholinergic neuroblastoma cell line Neuro-2a (ATCC no. CCL-131) (38, 42, 43). Neuro-2a cells were grown on 75-cm^2 tissue culture flasks in Eagle's minimum essential medium with Earle's salt containing 2 mM L-glutamine, 1.5 g/l sodium bicarbonate, 0.1 mM nonessential amino acids, 1.0 mM sodium pyruvate, and 10% FBS at 37°C in an atmosphere of 5% CO_2 and 95% air. Neuro-2a cells then were seeded at a density of $\approx 0.5 \times 10^5$ cells per well in a 24-well tissue culture plate. After incubation for 48 h, the media were removed and replaced with serum-free media, and the cells were grown for an additional 24 h. Next, the media were removed and replaced with serum-free media containing 2.0 μg of BoNT/A (Metabiologics Inc., Madison, WI) and varying concentration of inhibitor. After incubation for $\approx$48 h, the cells were harvested by removing the media, adding 80 μl of 1× NuPAGE LDS sample buffer (Invitrogen, Carlsbad, CA), and boiling for 10 min.

Western Blot Analysis. Proteins within the whole-cell extract samples were separated by SDS/PAGE on a 12% Bis-Tris NuPAGE gel in Mops/SDS running buffer (Invitrogen) before transfer to a 0.2 μm nitrocellulose membrane for 120 min at 30 V (38, 42, 43). After blocking in 2% skim milk/H_2O for 20 min at room temperature, the membrane was washed three times for 5 min at room temperature with TBST [25 mM Tris (pH 7.4), 137 mM NaCl, 2.7 mM KCl, and 0.1% (vol/vol) Tween 20]. Primary antibody, anti-SNAP-25 mouse monoclonal IgG_1 (200 μg/ml; Santa Cruz Biotechnology, Santa Cruz, CA) diluted 1:1,000 into 2% skim milk/H_2O, was added, and the blot was incubated for 20 min at room temperature followed by four 5-min washes with TBST at room temperature. Next, secondary antibody, goat anti-mouse HRP-conjugated (10 μg/ml; Pierce, Rockford, IL) diluted 1:500 into 2% skim milk/H_2O, was added, and the blot was incubated for 1 h at room temperature followed by washing for 90 min at room temperature. Bands were visualized with 4 ml of Super-Signal West Dura Chemiluminescent Substrate (Pierce) and analyzed with a FluorChem 8900 imager (Alpha Innotech, San Leandro, CA). Quantitation of the Western blot analysis was conducted by densitometric analysis.

Animal Studies. ***Preparation of* C. botulinum *type A neurotoxin.*** Type A neurotoxin was purified to a single 150-kDa component according to the method of Malizio *et al.* (44). The specific toxicity of the preparation was determined to be 3.5×10^8 mouse i.p. LD_{50}/mg of protein by a combination of the methods of Schantz and Kautter (45) and Boroff and Fleck (46). Neurotoxin was diluted to challenge dose levels in phosphate-buffered gelatin [30 mM sodium phosphate, 0.2% gelatin (pH 6.2)].

In vivo *assay.* Female CD-1 outbred mice (17–23 g; Harlan Sprague Dawley, Madison, WI) used in inhibition analyses were injected intravenously into the left-hand lateral tail vein with 0.1 ml of a solution of inhibitor (1.0 or 2.5 mM) solubilized in PBS/DMSO (9:1). After i.v. injection of inhibitor, animals that were included in the toxin challenge group were injected immediately with 0.5 ml of a solution of neurotoxin containing 5–10 i.p. LD_{50}/ml. Inhibitor control animals did not receive toxin challenge. Toxin control animals did not receive any compound before toxin challenge. Animals were observed for signs of botulism overnight, and the time of death in minutes was recorded.

We thank Joel Goldberg, Carl-Magnus Andersson, Romyr Dominique, and H. Y. Chou-Park for library preparations. This work was supported by National Institutes of Health Grants AI066507 (to K.D.J.) and CA78045 (to D.L.B.), National Institute of Allergy and Infectious Diseases (NIAID) Food and Waterborne Diseases Integrated Research Network Contract No. N01-AI-30050, the NIAID-sponsored "Great Lakes" Regional Center of Excellence (E.A.J.), and The Skaggs Institute for Chemical Biology. L.M.E. is a National Institutes of Health Postdoctoral Fellow (AI062014).

1. Johnson EA, Bradshaw M (2001) *Toxicon* 39:1703–1722.
2. Lacy DB, Tepp W, Cohen AC, DasGupta BR, Stevens RC (1998) *Nat Struct Biol* 5:898–902.
3. Hanson MA, Stevens RC (2000) *Nat Struct Biol* 7:687–692.
4. Singh BR (2000) *Nat Struct Biol* 7:617–619.
5. Schantz EJ, Johnson EA (1992) *Microbiol Rev* 56:80–99.
6. Johnson EA (1999) *Annu Rev Microbiol* 53:551–575.
7. Truong DD, Host WH (2006) *Parkinsonism Relat Disord* 12:331–355.
8. Arnon SS, Schechter R, Maslanka SE, Jewell NP, Hatheway CL (2006) *N Engl J Med* 354:462–471.
9. Byrne MP, Smith LA (2000) *Biochimie* 82:955–966.
10. Dickerson TJ, Janda KD (2006) *ACS Chem Biol* 1:359–369.
11. Hicks RP, Hartell MG, Nichols DA, Bhattacharjee AK, van Hamont JE, Skillman DR (2005) *Curr Med Chem* 12:667–690.
12. Boldt GE, Kennedy JP, Hixon MS, McAllister LA, Barbieri JT, Tzipori S, Janda KD (2006) *J Comb Chem* 8:513–521.
13. Boldt GE, Kennedy JP, Janda KD (2006) *Org Lett* 8:1729–1732.
14. Schmidt JJ, Stafford RG (2002) *FEBS Lett* 532:423–426.
15. Park JG, Sill PC, Makiyi EF, Garcia-Sosa AT, Millard CB, Schmidt JJ, Pang YP (2006) *Bioorg Med Chem* 14:395–408.

16. Burnett JC, Ruthel G, Stegmann CM, Panchal RG, Nguyen TL, Hermone AR, Stafford RG, Lane DJ, Kenny TA, McGrath CF, *et al.* (November 8, 2006) *J Biol Chem*, 10.1074/jbc.M608166200.
17. Adler M, Dinterman RE, Wannemacher RW (1997) *Toxicon* 35:1089–1100.
18. Adler M, Capacio B, Deshpande SS (2000) *Toxicon* 38:1381–1388.
19. Breidenbach MA, Brunger AT (2004) *Nature* 432:925–929.
20. Boger DL (2003) *Bioorg Med Chem* 11:1607–1613.
21. Boger DL, Desharnais J, Capps K (2003) *Angew Chem Int Ed* 42:4138–4176.
22. Dickerson TJ, Beuscher AE, IV, Rogers CJ, Hixon MS, Yamamoto N, Xu Y, Olson AJ, Janda KD (2005) *Biochemistry* 44:14845–14853.
23. Xu Y, Shi J, Yamamoto N, Moss JA, Vogt PK, Janda KD (2006) *Bioorg Med Chem* 14:2660–2673.
24. Lo Conte L, Chothia C, Janin J (1999) *J Mol Biol* 285:2177–2198.
25. Stites WE (1997) *Chem Rev* 97:1233–1250.
26. Jones S, Thornton JM (1996) *Proc Natl Acad Sci USA* 93:13–20.
27. Lawrence MC, Colman PM (1993) *J Mol Biol* 234:946–950.
28. Bogan AA, Thorn KS (1998) *J Mol Biol* 280:1–9.
29. Hu Z, Ma B, Wolfson H, Nussinov R (2000) *Proteins* 39:331–342.
30. Ma B, Wolfson HJ, Nussinov R (2001) *Curr Opin Struct Biol* 11:364–369.
31. DeLano WL (2002) *Curr Opin Struct Biol* 12:14–20.
32. Cheng S, Comer DD, Williams JP, Myers PL, Boger DL (1996) *J Am Chem Soc* 118:2567–2573.
33. Baldwin MR, Bradshaw M, Johnson EA, Barbieri JT (2004) *Protein Expr Purif* 37:187–195.
34. Binz T, Blasi J, Yamasaki S, Baumeister A, Link E, Sudhof TC, Jahn R, Niemann H (1994) *J Biol Chem* 269:1617–1620.
35. Keller JE, Neale EA, Oyler G, Adler M (1999) *FEBS Lett* 456:137–142.
36. Lipinski CA, Lombardo F, Dominy BW, Feeney PJ (2001) *Adv Drug Deliv Rev* 46:3–26.
37. Hatheway CH, Snyder JD, Seals JE, Edell TA, Lewis GE, Jr (1984) *J Infect Dis* 150:407–412.
38. Yowler BC, Kensinger RD, Schengrund C-L (2002) *J Biol Chem* 277:32815–32819.
39. Neale EA, Bowers LM, Jia M, Bateman KE, Williamson LC (1999) *J Cell Biol* 147:1249–1260.
40. Lalli G, Herreros J, Osborne SL, Montecucco C, Rossetto O, Schiavo G (1999) *J Cell Sci* 112:2715–2724.
41. Benatar MG, Willison HJ, Vincent A (1997) *J Neuroimmunol* 80:1–5.
42. Eubanks LM, Dickerson TJ, Janda KD (2005) *FEBS Lett* 579:5361–5364.
43. Boldt GE, Eubanks LM, Janda KD (2006) *Chem Commun* 29:3063–3065.
44. Malizio CJ, Goodnough MC, Johnson EA (1999) in *Methods in Molecular Biology*, eds Walker J, Holst O (Humana Press, Totowa, NJ), pp 27–39.
45. Schantz E, Kautter D (1978) *J Assoc Off Anal Chem* 61:96–99.
46. Boroff DA, Fleck U (1966) *J Bacteriol* 92:1580–1581.
47. Boger DL, Fink BE, Hedrick MP (2000) *J Am Chem Soc* 122:6382–6394.
48. Boger DL, Goldberg J, Jiang W, Chai W, Ducray P, Lee JK, Ozer RS, Andersson C-M (1998) *Bioorg Med Chem* 6:1347–1378.
49. Boger DL, Goldberg J, Satoh S, Ambroise Y, Cohen SB, Vogt PK (2000) *Helv Chim Acta* 83:1825–1845.